Theory and Theory-Based Models for the Pedestal, Edge Stability and ELMs in Tokamaks

P. N. Guzdar 1), S. M. Mahajan 2), Z. Yoshida 3), W. Dorland 1), B. N. Rogers 4), G. Bateman 5), A. H. Kritz 5), A. Pankin 5), I. Voitsekhovitch 5)[1], T. Onjun 5), S. Snyder 5)

1) IREAP, University of Maryland, College Park, MD, USA
2) IFS, University of Texas at Austin, Austin, TX, USA
3) Institute of Frontier Sciences, University of Tokyo, Tokyo, JAPAN
4) Department of Physics and Astronomy, Dartmouth College, Hanover, NH, USA
5) Lehigh University Physics Department, Bethlehem, PA USA

E-mails: guzdar@glue.umd.edu, bateman@lehigh.edu

Abstract: Theories for equilibrium and stability of H-modes, and models for use within integrated modeling codes with the objective of predicting the height, width and shape of the pedestal at the edge of H-mode plasmas in tokamaks, as well as the onset and frequency of Edge Localized Modes (ELMs), are developed. A theory model for relaxed plasma states with flow, which uses two-fluid Hall-MHD equations, predicts that the natural scale length of the pedestal is the ion skin depth and the pedestal width is larger than the ion poloidal gyro-radius, in agreement with experimental observations. Computations with the GS2 code are used to identify micro-instabilities, such as electron drift waves, that survive the strong flow shear, diamagnetic flows, and magnetic shear that are characteristic of the pedestal. Other instabilities on the pedestal and gyro-radius scale, such as the Kelvin-Helmholtz instability, are also investigated. Time-dependent integrated modeling simulations are used to follow the transition from L-mode to H-mode and the subsequent evolution of ELMs as the heating power is increased. The flow shear stabilization that produces the transport barrier at the edge of the plasma reduces different modes of anomalous transport and, consequently, different channels of transport at different rates. ELM crashes are triggered in the model by pressure-driven ballooning modes or by current-driven peeling modes.

1. Introduction

Tokamak plasmas undergo a spontaneous self-organizing transition from a low (L-mode) to a high confined state (H-mode) [1] when the heating power exceeds a critical value. The improved confinement is believed to be caused by the generation of a shear (zonal) flow, which is responsible for suppressing fluctuations and inhibiting transport. After this transition, a very steep pressure gradient develops at the edge. The height of the pressure pedestal is a natural figure of merit for energy confinement. Elucidation of the physics of pedestal formation, and predicting its maximum achievable height are issues crucial for magnetic fusion devices [2, 3]. Thus in this paper we present a model determining the pressure pedestal width and maximum height for the double Beltrami H-mode equilibrium restricted by ideal ballooning stability. Additional microinstabilities of H mode plasmas which survive the shear-flow stabilization investigated using analytical theory and the GS2 code are also presented. Finally, results from two variations of an edge model developed for use within integrated modeling codes with the objective of predicting the height, width and shape of the pedestal at the edge of H-mode plasmas, as well as the onset and frequency of Edge Localized Modes (ELMs), will be presented.

[1] Present address: Euratom/UKAEA, Abingdon, OX14 3DB, UK

2. Double-Beltrami equilibrium for H-mode

The theory of Mahajan and Yoshida [4] for the H-mode layer is extended to determine specifically the scalings of the pedestal height and width with plasma parameters. The centerpiece of this enterprise is the so-called double-Beltrami states (DB) obtained by the interaction of the magnetic and velocity fields. Under well-defined conditions [4], the self-organized DB state provides a description for the edge region of the H-mode plasma.

Starting with two-fluid Hall MHD equations in one-dimensional slab geometry (along the radial direction denoted by x), the solution for the magnetic fields and the flow in the edge boundary layer are given by [4]

$$B_{s,z} = -B_* Cos(\frac{\pi x}{2\lambda_i}) \tag{1}$$

$$B_{s,y} = (1 + \frac{4}{\pi^2})^{1/2} B_* Sin(\frac{\pi x}{2\lambda_i}) \tag{2}$$

$$V_y = \frac{2}{\pi}\frac{B_*}{B_0} V_A Sin(\frac{\pi x}{2\lambda_i}) \tag{3}$$

The total pressure is related to the magnetic field by the pressure balance condition

$$p + \frac{B_{s,z} B_0}{4\pi} = 0 \tag{4}$$

Here, λ_i=c/ω_{pi} is the ion skin-depth. Equations (1)-(4) form an explicit and complete solution except for a single undetermined quantity; the magnitude B_* of the magnetic field or equivalently the plasma pressure at the top of the pedestal. To determine this it is stipulated that the H-mode state maximizes the pressure gradient consistent with the ballooning stability criterion,

$$\frac{8\pi q^2 R}{B_0^2}\frac{dp}{dx} = \alpha_c \tag{5}$$

where q is the plasma safety factor R, the major radius and the parameter α_c contains the plasma shaping effects [3] in determining the stability of these modes. The pressure pedestal height expressed as pedestal β, then, is

$$\beta_{ped} = \frac{2\alpha_c}{\pi}\frac{\lambda_i}{q^2 R} = 2\frac{B_*}{B_0} \tag{6}$$

with the pedestal width Δ_{ped} given by

$$\Delta_{ped} = \lambda_i \tag{7}$$

Next we make quantitative comparisons of the pedestal height and width (if available) with three machines using data in published literature. However before we do so we cast the pedestal width and pedestal height into practical units which can facilitate comparison with data. The pedestal width (in meters) is given by

$$\Delta_{ped} = \frac{0.023}{Z}(\frac{A_H}{n_{ped}})^{1/2} \tag{8}$$

and the sum of the ion and electron temperatures (in keV) is

$$T_{e,ped} + T_{i,ped} = 0.36\frac{\alpha_c A_H^{1/2} B_T^2}{Z q^2 R n_{ped}^{3/2}} \tag{9}$$

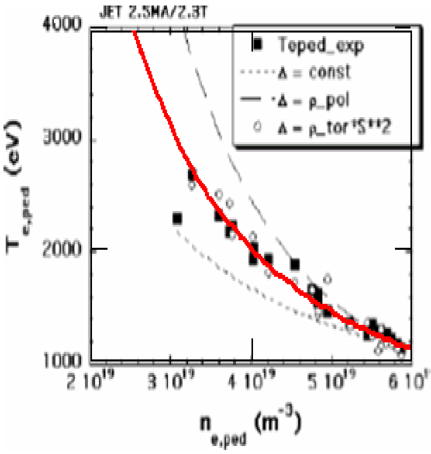

FIG. 1. $T_{e,ped}$ for experimental points (black squares), for model with constant pedestal width (dotted line), for model with pedestal width proportional to larmor radius (dashed line), for Sugihara model for pedestal width (open circles), for theory (red line) versus n_{ped} for JET discharges

The density is normalized to $10^{20}/m^3$, the major radius is in meters and the magnetic field in Tesla. Z is the ionic charge and A_H is the ion atomic mass relative to hydrogen. The first comparison is with data from JET [5, 6]. The data is for discharges with high elongation and triangularity and $I_P = 2.5\ MA$ and $B_T = 2.3\ T$. All these discharges displayed type I ELMy behavior. In Fig. 1, the black squares are experimental data points, the dotted and dashed curves show the pedestal temperature for constant pedestal width and for pedestal width scaling with the Larmor radius scale width respectively. The open circles are for the pedestal width given by the Sugihara model [5]. Since the data set does not include the ion temperature, we have assumed that the electron and ion temperatures are equal. This is expected to be true for the high density discharges but not so for the lower density cases. The solid line is a fit to the data for $\alpha_c/q^2 = 0.9$ using Equation (9). If q=2.5 at the top of the pedestal then $\alpha_c = 7$. This is consistent with ballooning mode stability studies which indicate that for low elongation and triangularity $\alpha_c = 3-4$, while for high elongation and triangularity $\alpha_c = 6-8$.

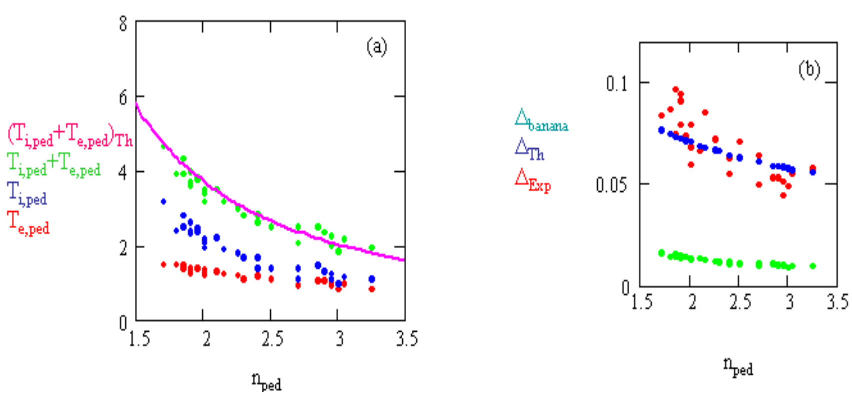

FIG. 2. (a) Data points $T_{e,ped}$(red), $T_{i,ped}$(blue), $T_{e,ped}$ + $T_{i,ped}$(green) Theory ($T_{e,ped}$ + $T_{i,ped})_{Th}$(magenta line) versus n_{ped}, (b) Pedestal width Δ, data(red), theory(blue), banana-width(green) versus n_{ped} for JT-60U discharges

In Fig. 2(a) and (b) is shown data from JT-60U [7] and its comparison with the theory. For these Type I ELMing discharges, $I_p = 1.8\ MA$ and $B_T = 3\ T$. These discharges had small elongation and triangularity. In Fig. 2(a) the temperature at the top of the pedestal is plotted as a function of the pedestal density. The red points are the electron temperature while the blue points are the ion temperature. The green points are the sum of the ion and electron temperatures at the top of the pedestal. The magenta curve is a fit to the data using $\alpha_c/q^2 = 0.22$ in Equation (29). If we assume that q=3.5 at the pedestal height, then $\alpha_c = 2.7$ which is a low value to be expected for these low elongation and low triangularity discharges. What is clearly seen from the data is that the electron and ion temperatures at the top of the pedestal are equilibrated for the high density discharges but not for the low density ones. Plotted in Fig. 2(b) are the experimental pedestal width (red points), the theoretical pedestal width (blue points) given by Equation (8), and the banana width (green points) as a function of the pedestal density.

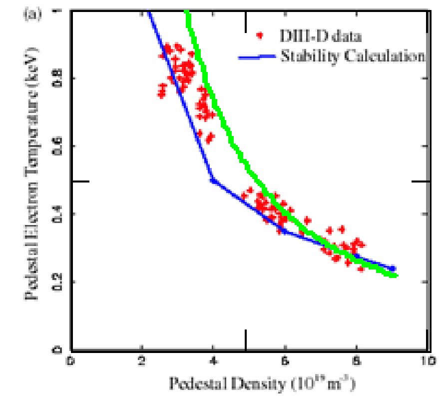

FIG. 3. $T_{e,ped}$ for experimental points (red crosses), for ballooning-peeling stability theory (blue line) and for theory (green line) versus n_{ped} for DIII-D discharges

Finally in Figure (3) the theory is compared with data from DIII-D. The red crosses are the experimental data for DIII-D discharges in the Type I ELM regime with $I_p = 1.225$ MA and $B_T = 2$ T [8]. The blue curve is based on a ballooning stability calculation of the discharges using the ELITE code. Once again since the ion temperature is not known we have assumed that the electron and ion temperatures are equal. Using Equation (9) with $\alpha_c/q^2 = 0.31$, yields the green theory curve.

3. Stability of H-mode pedestal to non-curvature driven modes

In this section we address the linear stability of simple slab plasma configurations without magnetic curvature using gyrokinetic simulations based on the GS2 code as well as analytic calculations. The configurations are characterized by sheared $\mathbf{E}\times\mathbf{B}$ and diamagnetic flows, weak collisionality, and finite magnetic shear, and are intended to model some of the salient features of the H-mode edge pedestal. Here we provide only a basic summary of the main results from a longer article [9].

Our simulations indicate the potential importance of at least three instabilities: the Kelvin-Helmholtz instability, the tertiary mode [10], and a non-local driftwave instability. These instabilities are all global modes, in the sense that they are all fundamentally dependent on non-local variations of the background "equilibrium" quantities, and are all absent from local simulations in which the background plasma gradients and the $\mathbf{E}\times\mathbf{B}$ shear V_E' (if present) are spatially constant. We now summarize some of our main results in each case.

3.1. Kelvin-Helmholtz instability

The Kelvin-Helmholtz instability is potentially the strongest instability of the three modes. In the absence of magnetic shear and ion diamagnetic effects the most unstable eigenmode has a typical growth rate $\gamma \sim V_E/\Delta$ (Δ is the total pedestal width) for a wavenumber $k \sim 1/\Delta$ in the direction of V_E. In the presence of magnetic shear, however, the mode can be stabilized if the pedestal width Δ is sufficiently wide. Assuming $L_s = qR/\hat{s}$ and $V'_{E,max} = 2V_E/\Delta$ (Δ=full pedestal width) this stability condition may be written as:

$$\Delta \gtrsim 1.6\rho_i \left(\frac{qR}{d_i\hat{s}}\frac{V_E}{V_{*i0}}\right)^{1/2} \quad (stable) \tag{10}$$

Here $d_i = c/\omega_{pi}$ is the ion skin depth and $V_{*i0} = 2\rho_i V_{thi}/\Delta$ is the typical ion diamagnetic velocity in the pedestal. Evaluating this condition for typical H-mode edge parameters in

DIII-D and Alcator CMOD yields a marginally stable pedestal width $\Delta_{crit} \sim 10\rho_i$. The similarity of this to observed values implies the Kelvin-Helmholtz instability in the H-mode edge is in fact near marginal stability due to the magnetic shear alone. Our analysis shows, however, that there is also another potentially important stabilizing factor in the H-mode edge, namely, ion diamagnetic effects. In the most unstable case of $k_\parallel = 0$ (no magnetic shear), ion diamagnetic effects alone can stabilize the mode if the ion diamagnetic velocity V_{*i} is at least comparable in magnitude to the $\mathbf{E}\times\mathbf{B}$ flow V_E and in the opposite direction. Typical edge profiles in experiments, as well as numerical simulations, suggest that such a balance, or partial balance, may indeed apply. Our final conclusion is therefore that the Kelvin-Helmholtz instability is suggestively close to marginal stability in the H-mode edge but that a more detailed comparison of simulations to experiments is needed to determine its actual role.

3.2. Tertiary mode

The tertiary mode, in contrast to the Kelvin-Helmholtz instability, arises at high-$k_\parallel$ and is characterized by an adiabatic electron response. It is driven by the ion temperature gradient, is radially localized by the $\mathbf{E}\times\mathbf{B}$ shear, and is insensitive to the magnetic shear. The equilibrium density gradient, discussed in detail in Ref. [9], also plays a complex role. Assuming the $\mathbf{E}\times\mathbf{B}$ velocity V_E and the ion diamagnetic velocity V_{*i} are comparable in magnitude, it has a typical radial width $\sim \sqrt{\rho_s \Delta}$, a growth rate $\gamma \sim (\rho_s/\Delta)^{1/2} V_E/\Delta$ that is smaller than that of the Kelvin-Helmholtz mode, and a frequency $\omega \simeq kV_E$. According to the GS2 simulations, this mode can be stabilized by finite Larmor radius (FLR) effects when $\Delta \sim (5-10)\rho_i$. Since the widths of experimental edge profiles typically approach this range, the tertiary mode in the edge region, like the Kelvin-Helmholtz instability, is a potentially important mode in the H-mode edge. A more detailed study is planned.

3.3. Drift wave instability

The nonlocal driftwave instability is a linear, edge-global version of a nonlinear driftwave mode that has been widely studied in local turbulence simulations of the edge region [11]-[14]. These turbulence simulations are typically carried out in the presence of spatially constant plasma gradients and magnetic shear, and as is well known [15], radially localized, linearly unstable driftwave eigenmodes do not exist in such systems. Nonlinearly, however, driftwave physics is hypothesized to play an important role in driving small-scale turbulence at H-mode-like parameters in the edge region, where resistive ballooning modes are expected to become weak [11]-[14]. We find here that in the presence of more realistic pedestal-like profiles in either the $\mathbf{E}\times\mathbf{B}$ velocity and/or the density gradient, a robustly unstable, radially localized linear eigenmode reappears in the simulations, with or without magnetic shear. This result is consistent with past theoretical studies of driftwaves going back for decades, which have shown that strong spatial variations in the density gradient [16]-[20] can overcome the damping introduced by magnetic shear. Here, to obtain a theoretical description of the mode that is in reasonable agreement with the GS2 simulations for edge-like parameters, we needed to go beyond past work and include in our analytic calculations the contributions from electron Landau damping, electromagnetic effects, as well as the spatial variation in the $\mathbf{E}\times\mathbf{B}$ velocity, density and temperature profiles. Including these effects and considering the simplest case of quasi-local modes with $k\Delta \gg 1$, the linear eigenfunction becomes a simple Gaussian with radial mode width $\sqrt{\Delta/k} < \Delta$. Typical maximum growth rates are $\gamma_{max} \sim (0.1-0.2)\omega_{*e,n}$ for $k_\parallel \sim \sqrt{\beta} k\rho_s/\Delta$. Since the mode remains robustly unstable down relatively large scale lengths $k \sim 1/\Delta$ despite the presence of $\mathbf{E}\times\mathbf{B}$ and magnetic shear, our conclusion in this case is that the drift-wave mode seems to be a strong candidate for driving anomalous transport in the H-mode edge of either toroidal or linear confinement devices.

4. Integrated modeling of the pedestal and ELMs

Two variations of an edge model have been developed for use within integrated modeling codes with the objective of predicting the height, width and shape of the pedestal at the edge of H-mode plasmas in tokamaks, as well as the onset and frequency of Edge Localized Modes (ELMs).

One version of the edge model has been implemented in the JETTO code [21]. In the JETTO model, the ion thermal neoclassical diffusivity is used to compute all the channels of transport within the pedestal. The MHD stability criterion that triggers ELM crashes is calibrated in each simulation using the HELENA and MISHKA stability codes. Simulations of a JET triangularity scan using this model reproduce the experimentally measured pressure profiles and demonstrate a transition from first to second stability as the triangularity of the plasma is increased [22], and simulations of a JET power scan show that the pedestal height and ELM frequency increase with increasing heating power as observed in the experiment [23]. In some of the JETTO simulations, it is shown that there is a transition from ELMs that are initially triggered by pressure-driven ballooning modes to ELMs triggered by current-driven peeling modes [24]. Recent simulations of a deuterium to tritium isotope scan with the JETTO model have produced quantitative agreement with experimental data for the pedestal height and ELM frequency.

A new edge model has been developed and implemented in the ASTRA code to predict the width and shape of the pedestal in addition to the pedestal height and the ELM frequency [25]. In this model, the anomalous thermal transport driven by long wavelength ion drift modes (ITG/TEM) is reduced by flow shear, which reduces the electron thermal transport to values that are close to the transport driven by electron temperature gradient (ETG) modes and reduces the ion thermal transport to values that are close to neoclassical transport. The main contributions to the electron and ion thermal diffusivities (χ_e and χ_i) are

$$\chi_e = \frac{\chi_e^{\mathrm{ITG/TEM}}}{1 + C^{\mathrm{ITG/TEM}}(\omega_{E\times B}\tau^{\mathrm{ITG/TEM}})^2} + \chi_e^{\mathrm{ETG}} \tag{11}$$

$$\chi_i = \frac{\chi_i^{\mathrm{ITG/TEM}}}{1 + C^{\mathrm{ITG/TEM}}(\omega_{E\times B}\tau^{\mathrm{ITG/TEM}})^2} + \chi_i^{\mathrm{neoclassical}} \tag{12}$$

where $\chi_{e,i}^{\mathrm{ITG/TEM}}$ are the electron and ion thermal diffusivities computed using the Weiland model for ion drift modes [26], $C^{\mathrm{ITG/TEM}}$ is a calibration coefficient for the fow shear stabilization, $\omega_{E\times B}$ is the flow shear rate, $\tau^{\mathrm{ITG/TEM}}$ is the turbulence correlation time, which is estimated to be the reciprocal of the fastest ion drift mode growth rate, χ_e^{ETG} is the electron thermal diffusivity driven by ETG modes, and $\chi_i^{\mathrm{neoclassical}}$ is the ion thermal neoclassical diffusivity. ELM crashes are triggered whenever the pressure gradient anywhere within the pedestal exceeds the critical pressure gradient for short-wavelength ballooning modes

$$2\mu_0 R(q/B)^2(dp/dr) > 0.4s[1 + \kappa_{95}^2(1 + 5\delta_{95}^2)] \tag{13}$$

or whenever the current density anywhere within the pedestal exceeds the peeling mode stability criterion (which is also a function of the pressure gradient) [27]

$$C_k \left[1 + \frac{1}{\pi q'(\psi)} \oint \frac{\mu_0 J_\parallel B}{R^2 B_p^3} d\ell\right] > \sqrt{1 - 4D_m}. \tag{14}$$

In these relations, R and r are the major and minor radius, q is the safety factor, B and B_p are the toroidal and poloidal magnetic field, p is the thermal pressure, D_m is the Mercier coefficient, which is proportional to the pressure gradient, C_k is a coefficient that is introduced to reproduce the effects of the vacuum region and plasma shaping, ψ is the poloidal flux, and $J_{\|}$ is the parallel plasma current density. When each ELM crash occurs, the edge profiles are changed instantaneously on the transport time scale, and then the pedestal profiles rebuild as a result of the flow shear stabilization during the remainder of the ELM cycle [25].

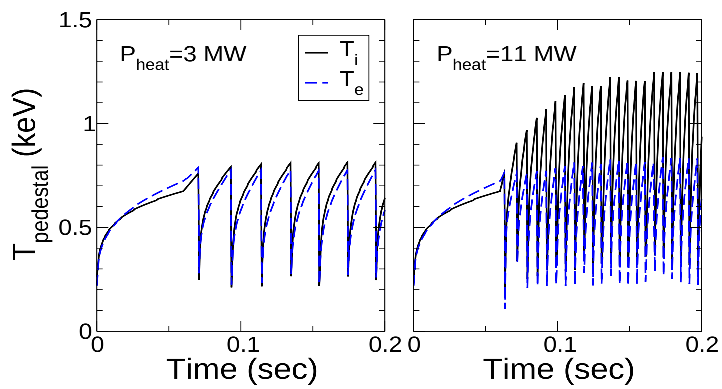

FIG. 4. Time evolution of the ion and electron temperature at the top of the pedestal for a low power (left panel) and high power (right panel) discharge using typical DIII-D parameters.

As the heating power in a simulation is increased as a function of time, the model predicts a transition from L-mode to H-mode, with the formation of an edge transport barrier and resulting pedestal at the edge of the H-mode plasma. As the heating power is increased further, there is a transition from an ELM-free H-mode to a type I ELMy H-mode, as shown in Fig. 1. It can be seen in Fig. 4 that the ELM frequency increases with increasing heating power, which is a characteristic of type I ELMs. In addition, the ion temperature at the top of the pedestal increases moderately with increasing heating power ($T_i^{\text{ped}} \propto$ (heating power)$^{0.3}$), which is consistent with experimental observations [28]. The scaling of the pedestal temperatures with magnetic field and plasma density are also consistent with experimental data [25]. During the calibration of this model against experimental data, it was observed that changes in the flow shear rate coefficient $C^{\text{ITG/TEM}}$ have little effect on the pedestal height or ELM frequency, once the coefficient is large enough. The stability criterion used to trigger ELM crashes, however, has a significant effect on the pedestal height and ELM frequency.

Summary

The present paper addresses the equilibrium, stability and integrated modeling of the edge region of H-mode plasmas. The double-Beltrami equilibrium state together with the ideal ballooning stability criterion yields a prediction for the pedestal width and height, which compare favorably with some observations on current machines. Linear drift-wave eigenmodes are found to be robustly unstable in the H-mode edge region despite ExB and magnetic shear effects. They are therefore potentially the main driver of transport in the (H-mode) edge of toroidal or linear devices. Finally results from two edge models, one using the JETTO code in combination with the HELENA and MISHKA stability codes which provide conditions for an ELM crash, and a second edge model using shear-flow modified transport coefficients implemented in the ASTRA code, have been presented. Good agreement of modeled ELM characteristics with observed behavior has been found, with strongest sensitivity to the stability criterion used to trigger ELM crashes.

Acknowledgments

Work supported by US Department of Energy under grant DE-FG02-93ER54197 at University of Maryland, grant DE-FG03-96ER54366 at University of Texas at Austin and grant DE-FG02-92ER-5414 at Lehigh University. PNG thanks Dr. Y. Kamada and Dr. H. Urano for providing JT-60U data.

References

[1] WAGNER, F., and ASDEX Team, Phys. Rev. Lett. **49** (1982) 1408.
[2] KOTHSCHENREUTHER, M., et al., in Plasma Phys. and Control. Nucl. Fusion Research (Proc. 16th Int. Conf. Montreal, 1996) Vol. 2, IAEA, Vienna (1997) 371.
[3] ONJUN, T., et al., Phys. Plasmas **9** (2002) 5018.
[4] MAHAJAN, S. M., YOSHIDA, Z., Phys. Plasmas **7** (2000) 635.
[5] SUGIHARA, M., et al., Nucl. Fusion, **40** (2000) 1743.
[6] LINGERTAT, J., et al., J. Nucl. Mater. **266-269** (1999) 124.
[7] URANO, H., et al. 27th EPS Conf. Plasma Phys. and Contr. Fusion, Budapest, 12-16 June 2000, ECA Vol **24B** (2000) 956.
[8] SNYDER, P. B., et al., Nucl. Fusion **44** (2004) 320.
[9] ROGERS, B. N., and DORLAND, W. submitted to Phys. of Plasmas (2004).
[10] ROGERS, B. N., et al, PRL, **85** (2000) 5336.
[11] DRAKE, J., et al, PRL **75** (1995) 4222.
[12] ZEILER, A., et al, Phys. Plasmas **3** (1996) 2951.
[13] SCOTT, B., D., Plasma Phys. Control. Fusion **39** (1997) 1635.
[14] ROGERS, B. N., et al, PRL, **81** (1998) 4396.
[15] ANTONSEN, T. M., Jr., Phys Rev. Lett. **41** (1978) 33.
[16] COPPI, B., Phys. Lett. **14** (1965) 172.
[17] KRALL, N., and ROSENBLUTH, M., Phys. Fluids **8** (1965) 1488.
[18] S. MOISEEV, S., and SAGDEEV, R., Sov. Phys.-Tech. Phys. **9**,196 (1964).
[19] TAYLOR, J. B., in Plasma Phys. and Control. Nucl. Fusion Research (Proc. 6th Int. Conf. Berchtesgaden, 1976) Vol. 2, IAEA, Vienna (1977) 323.
[20] CHEN, L., et al, Nucl. Fusion **19**, No. 3 (1979) 373.
[21] PARAIL, V., BATEMAN, G., BECOULET, M., et al., Plasma Physics Reports **29** (2003) 539.
[22] ONJUN, T., KRITZ, A. H., BATEMAN, G., et al., Phys. Plasmas. **11** (2004) 3006.
[23] ONJUN, T., KRITZ, A. H., BATEMAN, G., et al., Phys. Plasmas. **11** (2004) 1469.
[24] ONJUN, T., KRITZ, A. H., BATEMAN, G., et al., Interplay between ballooning and peeling modes in simulations of edge localized modes, 2004, to appear in Phys. Plasmas.
[25] PANKIN, A. Y., VOITSEKHOVITCH, I., BATEMAN, G., et al., Combined model for the H-mode pedestal and ELMs, 2004, submitted to Plasma Physics and Controlled Fusion.
[26] BATEMAN, G., KRITZ, A. H., KINSEY, J. E., REDD, A. J., and WEILAND, J., Phys. Plasmas **5** (1998) 1793.
[27] CONNOR, J., HASTIE, H., WILSON, H., and MILLER, R., Phys. Plasmas **5** (1998) 2687.
[28] CORDEY, J. G., for the ITPA H-mode Database Working Group, and the ITPA Pedestal Database Working Group, Nuclear Fusion **43** (2003) 670.